Double-pulsed carrier speckle-shearing pattern interferometry for transient deformation analysis

A. Fernández[a], A. F. Doval[a], A. Dávila[b], J. Blanco-García[a], C. Pérez-López[b], and J. L. Fernández[a]

[a] Universidade de Vigo, Departamento de Física Aplicada
ETSEIM Lagoas-Marcosende, 9. E-36200 Vigo (SPAIN)
Phone: +34 986 812 216, Fax: +34 986 812 201

[b] Centro de Investigaciones en Óptica, A. C.
Apartado Postal 1-948. 37150 León-Gto (MEXICO)
Phone: + 52 47 731 017, Fax: + 52 47 175 000

ABSTRACT

We report on a novel technique for the evaluation of transient phase in double-pulsed electronic speckle-shearing pattern interferometry. Our technique requires the acquisition of just two speckle-shear interferograms (one before and one after object's deformation) which are correlated by subtraction to obtain a fringe pattern. A spatial carrier is generated by means of an original optical setup based on the separation and later recombination of the two beams produced by a Nd:YAG twin pulsed laser. One introduces an optical path difference in the curvature radii of the illumination beams by mismatching the distances from two diverging lenses to a beam combiner. This procedure gives rise to a linear phase term in the second speckle-shear interferogram that plays the role of a spatial carrier and allows the use of spatial phase measurement methods to analyze the fringe pattern. We present the theoretical aspects of the technique as well as its experimental implementation.

Keywords: electronic speckle-shearing pattern interferometry, spatial carrier, transient deformation measurement, speckle metrology, shearography

1. INTRODUCTION

Electronic speckle-shearing pattern interferometry (ESSPI) is a nondestructive, whole-field technique that allows the measurement of displacement gradients. Early work on shearing techniques used moiré fringes resulting of the superposition of two fringe patterns obtained by holographic interferometry.[1] Later, photographic film has been replaced by electronic devices, avoiding the somewhat expensive and time-consuming development process.[2] Displacement gradients can also be obtained by the closely related electronic speckle pattern interferometry (ESPI) through image processing.[3] However, in applications that involve the measurement of displacement gradients, such as strain analysis or detection of local defects in various materials, ESSPI outstrips ESPI in several aspects. First, the calculation of spatial derivatives is a time-consuming operation, while ESSPI yields the displacement differences directly. Second, due to its quasi-common path design, ESSPI is less sensitive than ESPI to the influence of environmental disturbances, e.g., air turbulence, external vibration, rigid body motion, etc. Moreover, the requirement of a light source with large coherence length may be relaxed. And third, the possibility to change the sensitivity of the interferometer by adjusting the amount of shear broadens the measurement range of ESSPI.

The use of pulsed lasers in ESSPI relaxes even more the stability requirements for the experimental setup and makes possible the analysis of high-speed transient events. Nevertheless, only a few papers reporting on pulsed ESSPI have appeared. Spooren *et al.*[4] originally demonstrated the application of a double-pulsed laser to electronic speckle-shear interferometry. Shear is introduced in the speckle interferograms by slightly tilting one of the mirrors in a

Correspondence should be addressed to Antonio Fernández, e-mail: antfdez@uvigo.es

Michelson type of shear interferometer,[5] and correlation fringe patterns are formed by double-pulse subtraction,[6] a technique formerly proposed for ESPI. Emphasis was given to the study of fringe visibility rather than to the implementation of a phase evaluation method, and hence measurements are qualitative. The first quantitative measurements of displacement gradients with ESSPI have been carried out by Pedrini *et al.*[7] They use a Mach-Zehnder interferometer after the imaging lens in order to record the interference between two sheared images on a CCD. Lateral shear between these two images is adjusted by shifting one of the two mirrors in the setup. Spatial carrier is introduced in the speckle-shear interferograms by tilting one mirror (or one beam splitter). Interference phase is evaluated by either the Fourier transform[8] or the spatial-carrier phase-shifting[9] methods. The optical phase change due to object's deformation is obtained as the difference between two phase distributions calculated from two speckle-shear interferograms recorded before and after deformation, respectively. More recently, Dávila *et al.*[10] have performed quantitative measurements of transient displacement gradients with pulsed ESSPI following a different approach. Spatial carrier is introduced in the correlation fringe patterns rather than in the speckle-shear interferograms by translating manually the diverging lens that expands the illumination beam along its optical axis between two laser pulses, and phase is evaluated by the spatial synchronous detection method.[11] The technique has been experimentally demonstrated in laboratory conditions. Unfortunately, the long time required for the lens translation (several seconds) negates the advantages of pulsed ESSPI and prevents its application in industrial environments. Bonding the diverging lens to a piezoelectric translator significantly improves the immunity of the system to environmental disturbances. This solution has been adopted in a double-pulsed-addition ESPI system for harmonic vibration measurement.[12] However, it has been found that the use of a piezo-mounted lens to generate carrier fringes still imposes a lower limit to the minimum separation between laser pulses because of the response time of the piezoelectric element.

In this paper, we present a novel technique for quantitative measurement of the derivatives of displacement with double-pulsed ESSPI. We use a Michelson type of shear interferometer sensitive to displacements of the object normal to its surface (out of plane). Two speckle-shear interferograms are recorded with a CCD; the first one with the object at rest, and the second one after the object is stressed. Correlation fringes are formed by double-pulse subtraction.[6] Spatial carrier is introduced in the secondary correlation fringe patterns by changing the curvature radius of the illumination wavefront between laser pulses. The proposed technique is somewhat similar to the one described in ref. 10, but we present a new optical setup without moving devices and, therefore, the only lower limit to the minimum separation between laser pulses is imposed by the charge transfer period of the CCD (about 1 μs in an interline transfer CCD[13]).

2. PRINCIPLE OF DOUBLE-PULSED SUBTRACTION ESSPI WITH SPATIAL CARRIER

2.1. Fringe formation

A speckle-shear interferogram produced by a single laser pulse is formed by coherent superposition of two sheared speckle patterns. In double-pulsed subtraction ESSPI,[4] the CCD camera records two speckle-shear interferograms in separated video fields. The first laser pulse is fired with the object at rest, and the corresponding intensity distribution $I_1(\mathbf{x})$ on the image plane may be expressed as

$$I_1(\mathbf{x}) = I_m(\mathbf{x})\{1 + V(\mathbf{x})\cos[\psi(\mathbf{x})]\} \tag{1}$$

where $I_m(\mathbf{x})$ and $V(\mathbf{x})$ are the mean intensity and the visibility of the speckle-shear interferogram at a point $\mathbf{x} = (x,y)$ of the image plane, respectively, and $\psi(\mathbf{x})$ is the difference between the random phases of the interfering speckle patterns. Some time later (typically tens of microseconds) the object is stressed and the laser emits a second pulse properly timed with respect to the mechanical excitation. We denote the resulting speckle-shear interferogram by

$$I_2(\mathbf{x}) = I_m(\mathbf{x})\{1 + V(\mathbf{x})\cos[\psi(\mathbf{x}) + \phi(\mathbf{x})]\} \tag{2}$$

where $\phi(x,y)$ represents the deterministic optical phase increment due to the deformation of the object. Time dependence has been omitted in Eqs. (1) and (2) because of the extremely short pulse duration, that effectively freezes movement in each CCD exposure.

Subtraction of primary speckle-shear interferograms (1) and (2) and subsequent full wave rectification yields a speckled, high visibility, secondary correlation fringe pattern expressed by

$$I(\mathbf{x}) = |I_1(\mathbf{x}) - I_2(\mathbf{x})| = 2I_m(\mathbf{x})V(\mathbf{x})\left|\sin\left[\psi(\mathbf{x}) + \frac{\phi(\mathbf{x})}{2}\right]\sin\left[\frac{\phi(\mathbf{x})}{2}\right]\right| \quad (3)$$

In a shear interferometer, contributions from two object points separated by a distance Δx_o are received in the same image point **x**. Provided that the angle between the directions of illumination and observation is small, phase increment $\phi(\mathbf{x})$ in Eqs. (2) and (3) is given by[14]

$$\phi(\mathbf{x}) = \frac{2\,\partial p(\mathbf{x})}{\partial x}\Delta x = \frac{2\,\partial p(\mathbf{x})}{\partial x} M \Delta x_o \quad (4)$$

where λ is the wavelength of the laser light, and $p(\mathbf{x})$ is the variation of the optical path between laser pulses. The term Δx_o is called the object plane shear, and is related to the image plane shear Δx through the magnification of the imaging system M.

2.2. Spatial carrier generation

Our experimental setup for spatial carrier generation in double-pulsed ESSPI is shown in Fig. 1. The light source consists of two separate Q-switched Nd:YAG oscillators, commonly seeded by a diode-pumped Nd:YAG CW laser to obtain mutual coherence between their beams. The infrared outputs are combined at BC1 before passing through a frequency-doubling crystal that makes alignment and signal detection safer and easier. Moreover, the sensitivity of the interferometer is multiplied by a factor of two. Each cavity produces 12 mJ in 20-ns pulses at 532 nm at a rate of 25 Hz. Giving a small tilt to mirror M4, the green radiation produced by cavity 1 goes through a different path than light produced by cavity 2. Both beams are expanded through diverging lenses and then are made collinear at BC2. The lens NL2 is placed a distance d (exaggerated in the diagram for clarity) nearer to BC2 than NL1, and therefore the curvature radius of the illumination beam is greater for the first laser pulse than for the second. Thus the term $p(\mathbf{x})$ in Eq. (4) is due not only to out of plane displacement of the object's surface between pulses $w(\mathbf{x})$, but also to local variation of the optical path of the illumination wavefront $l(\mathbf{x})$ (see Fig. 2),

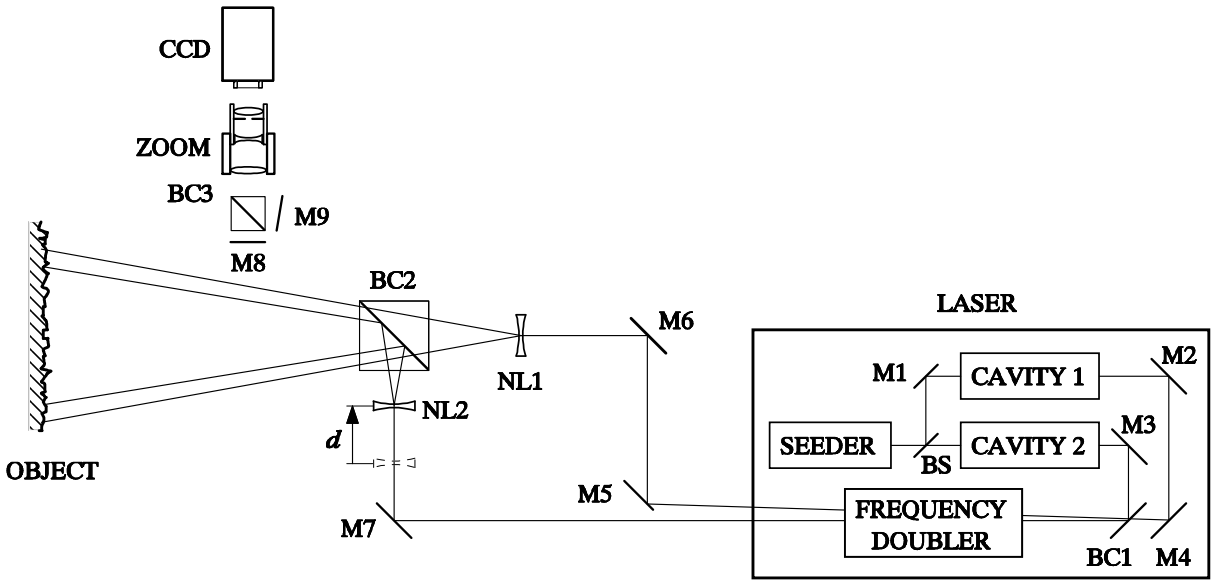

Fig. 1. Experimental setup for spatial carrier generation in double-pulsed ESSPI. The optical components are BS, beam splitter; BC1-BC3, beam combiners; M1-M9, mirrors; NL1 and NL2, negative lenses (their virtual foci are shifted by a distance d).

$$p(\mathbf{x}) = 2w(\mathbf{x}) + l(\mathbf{x}) \tag{5}$$

When the distance from the diverging lenses to the object is large enough, only paraxial rays are relevant, and the last term in Eq. (5) becomes[15]

$$l(\mathbf{x}) \approx \frac{x_o^2 + y_o^2}{2}\left(\frac{1}{R_2} - \frac{1}{R_1}\right) = \frac{x^2 + y^2}{2M^2}\left(\frac{1}{R_2} - \frac{1}{R_1}\right) \tag{6}$$

where the relationship $\mathbf{x} = M\mathbf{x}_o$ between image plane coordinates and object plane coordinates has been used again.

Substitution of Eqs. (5) and (6) in Eq. (4) makes apparent that the phase difference $\phi(\mathbf{x})$ is composed of two different contributions

$$\phi(\mathbf{x}) \approx \frac{4\ M\Delta x_o}{\partial x}\frac{\partial w(\mathbf{x})}{\partial x} + 2\underbrace{\frac{\Delta x_o}{M}\left(\frac{1}{R_2} - \frac{1}{R_1}\right)}_{f_c} x \tag{7}$$

The first term in Eq. (7) is proportional to the derivative along X direction of object's out of plane displacement, and the second term is the spatial carrier. If R_2 and R_1 are large compared to $d = R_1 - R_2$, we can make use of the approximation $R_1 \approx R_2 \approx R$ to express the carrier frequency in a more compact form

$$f_c \approx \frac{d\ \Delta x_o}{\lambda\ M\ R^2} \tag{8}$$

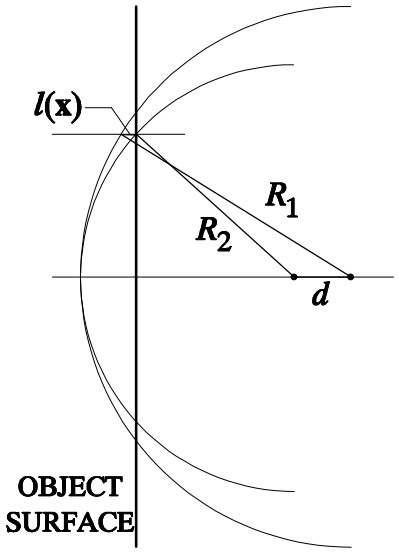

Fig. 2. Phase difference $l(\mathbf{x})$ due to a shift d of the virtual foci

3. EXPERIMENTAL RESULTS

We have demonstrated the optical arrangement schematically represented in Fig. 1 for the measurement of spatial derivatives of the out of plane component of transient bending waves, impact induced by applying a voltage pulse to a piezoelectric translator. Timing between piezo translator driving pulse and firing of the second laser pulse is adjusted by a programmable delay generator. The operation of our double-pulsed ESSPI system is as follows. The laser continuously emits twin-pulses at a rate of 25 Hz, properly timed with respect to the video signal. When the operator gives the order to start, the test object is impacted by the piezo translator and a video frame is digitized and stored as 512×515×8 bits in a frame grabber. The irradiance values recorded by the CCD during both first and second first laser pulses, Eqs. (1) and (2), are contained in the even lines and the odd lines of this image, respectively. Intensity fluctuations between first and second laser pulses are digitally compensated. Next, a frame processor subtracts even lines from the adjacent odd ones and rectifies the result, Eq. (3), yielding a set of equispaced vertical carrier fringes modulated by the displacement derivative. The interested reader is addressed to references 16 and 17 for further details on the synchronism.

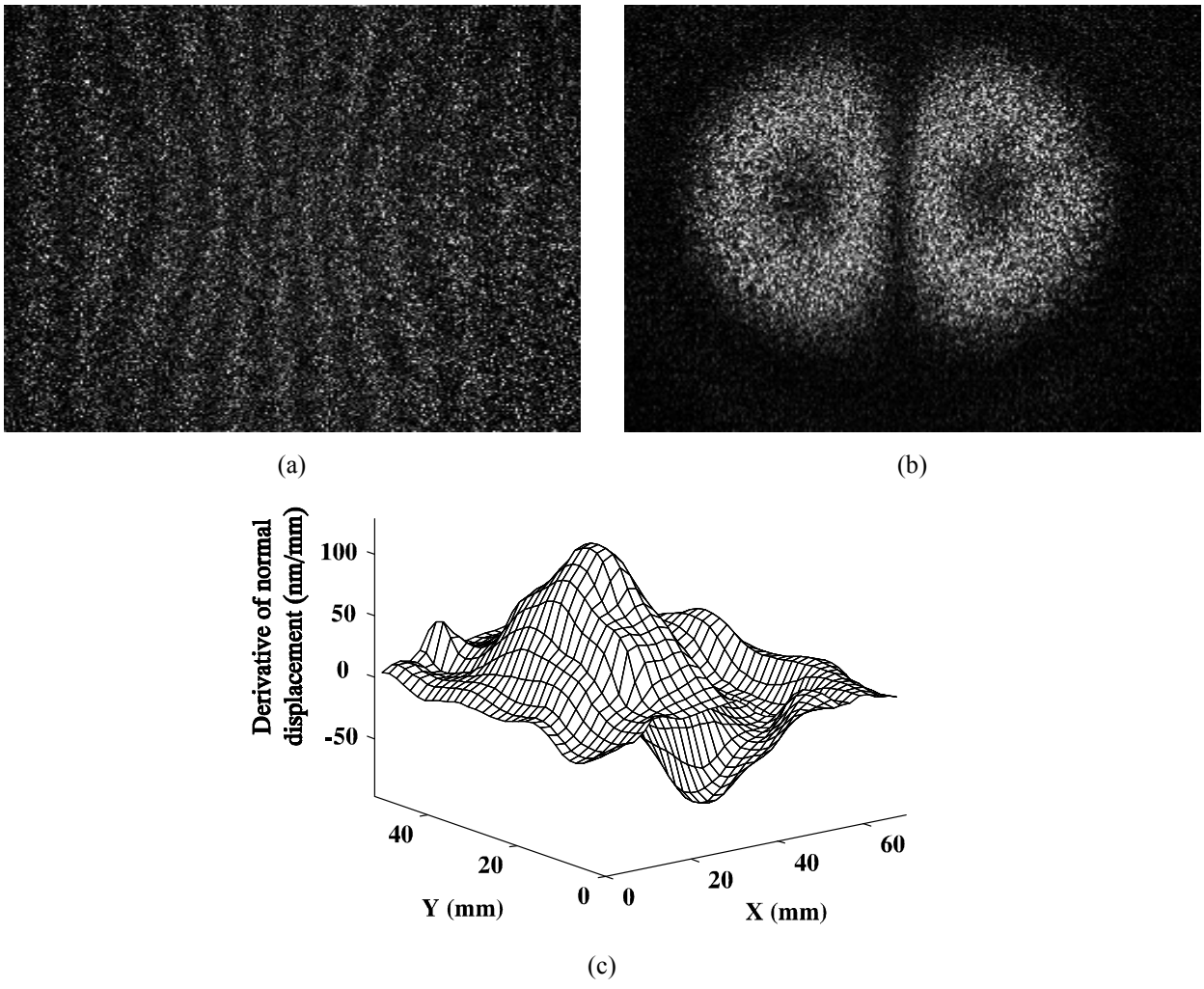

Fig. 3. Transient bending waves in an aluminium plate excited by impact. (a) Carrier fringes modulated by the spatial derivative of the out of plane displacement. (b) Modulation fringes obtained without carrier ($d = 0$). (c) Pseudo 3-D plot of $\partial w(\mathbf{x})/\partial x$

A detailed description of the analysis of ESSPI carrier fringes using the spatial synchronous detection (SSD) can be found elsewhere.[10] Therefore, only a brief account is given here. The ESSPI carrier fringes are previously filtered by a thresholded (power selective) Fourier filter, followed by low-pass (frequency selective) filter. As vertical carrier fringes have been used, the analysis proceeds by treating each of the 512 horizontal lines in isolation. The products of each filtered horizontal line $I'(x)_n$ of the ESSPI pattern with $\sin(2\pi f_c x)$ and $\cos(2\pi f_c x)$ are evaluated, the number of the horizontal line denoted by the subscript n. A low-pass filter is applied to isolate the phase term of the horizontal lines and the resulting filtered image lines $G_s(x)_n$ and $G_c(x)_n$ may then be processed to extract the wrapped phase $\phi_n(x)$ using the relation

$$\phi_n(x) = \tan^{-1}\left(\frac{G_s(x)_n}{G_c(x)_n}\right) \tag{9}$$

The last step in the phase evaluation procedure is carried out by applying an iterative cosine transform unwrapping algorithm[18] to the wrapped phase map represented by $\phi(\mathbf{x})$.

An application example is shown in Fig. 3. The specimen is an aluminum alloy plate of dimensions 300 mm ×120 mm × 3.5 mm (an area of approximately 70 mm × 52 mm was measured), clamped along the left and the right edges. Object plane shear was set to $\Delta x_o = 22$ mm. Fig. 3(a) is a fringe pattern, modulation plus carrier, obtained with a delay of 30 μs between object excitation and second laser pulse. For comparison purposes Fig. 3(b) shows a fringe pattern containing the same modulation than Fig. 3(a), but without spatial carrier. Finally, Fig. 3(c) shows a pseudo 3-D plot of the measured spatial derivative along the X direction of the out of plane transient displacement of the object's surface.

4. CONCLUSIONS

We have developed a double-pulsed ESSPI system for the measurement of spatial derivatives of out of plane displacements. The introduction of carrier fringes by mismatching the distances from the diverging lenses to the beam combiner allows quantitative analysis from a single fringe pattern. This makes our system particularly well suited for the analysis of transient events, e.g. bending waves induced by impact. By repeating the experiment with a varying time delay from the start of the transient event to the second laser pulse, it is possible to obtain a sequence of quantitative measurements which shows the temporal evolution of the measured magnitude. The SSD allows straightforward unambiguous evaluation of phase when a single fringe pattern is available. However, a knowlegde of the exact carrier frequency is required to avoid phase evaluation errors and the low-pass filters should be carefully adjusted to keep the phase measurement error small. Finally, our system is highly immune to external disturbances because of the short time separation between laser pulses (typically tens of microseconds). This is a valuable feature for the operation in industrial environments.

5. ACKNOWLEDGMENTS

This work was funded by the following companies and institutions: Xunta de Galicia (XUGA 32101B95), Comisión Interministerial de Ciencia y Tecnología (TAP97-0829-C03-01) and Universidade de Vigo. A. Fernández and J. Blanco-García are indebted to Ministerio de Educación y Cultura and Xunta de Galicia, respectively, for travel grants.

6. REFERENCES

1 P. Boone and R. Verbiest, "Application of hologram interferometry to plate deformation and translation measurements", Optica Acta 16 (5), pp. 555-567, 1969.

2 S. Nakadate, T. Yatagai, and H. Saito, "Digital speckle-pattern shearing interferometry", Applied Optics 19 (24), pp. 4241-4246, 1980.

3 E. Vikhagen, "Nondestructive testing by use of TV holography and deformation phase gradient calculation", Applied Optics 29 (1), pp.137-144, 1990.

4 R. Spooren, A. A. Dyrseth, and M. Vaz, "Electronic shear interferometry: application of a (double-) pulsed laser", Applied Optics 32 (25), pp. 4719-4727, 1993.

5 P. K. Rastogi, "Techniques of displacement and deformation measurements in speckle metrology", Speckle Metrology (Rajpal S. Sirohi Ed.), pp. 41-98, Marcel Dekker Inc., 1993.

6 R. Spooren, "Double-pulse subtraction TV holography", Optical Engineering 31 (5), pp. 1000-1007, 1992.

7 G. Pedrini, Y.-L. Zou, and H. J. Tiziani, "Quantitative evaluation of digital shearing interferogram using the spatial carrier method", Pure and Applied Optics 5, pp. 313-321, 1996.

8 M. Takeda, H. Ina and S. Kobayashi, "Fourier-transform method of fringe-pattern analysis for computer-based topography and interferometry", Journal of the Optical Society of America 72 (1), pp. 156-160, 1981.

9 M. Kujawinska, "Spatial phase measurement methods", Interferogram Analysis (D. W. Robinson and G. T. Reid Ed.), pp.141-193, IOP Publishing Ltd., 1993.

10 A. Dávila, G. H. Kaufmann, and C. Pérez-López, "Transient deformation analysis using a carrier method of pulsed electronic speckle-shearing pattern interferometry", Applied Optics (accepted 1998).

11 K. H. Womack, "Interferometric phase measurement using spatial synchronous detection", Optical Engineering 23 (4), pp. 391-395, 1984.

12 A. J. Moore and C. Pérez-López, "Fringe carrier methods in double-pulsed addition ESPI", Optics Communications 141, pp. 203-212, 1997.

13 G. C. Holst, CCD arrays, cameras and displays, Chap. 3, JCD Publishing and SPIE Optical Engineering Press, 1996.

14 R. S. Sirohi, "Speckle methods in experimental mechanics", Speckle Metrology (Rajpal S. Sirohi Ed.), pp. 99-156, Marcel Dekker Inc., New York, 1993.

15 J. W. Goodman, Introduction to Fourier Optics, Chap. 5, McGraw-Hill, San Francisco, 1968.

16 A. Fernández, A. J. Moore, C. Pérez-López, A. F. Doval, and J. Blanco-García, "Study of transient deformations with pulsed TV holography: application to crack detection", Applied Optics 36 (10), pp. 2058-2065, 1997.

17 A. Fernández, J. Blanco-García, A. F. Doval, J. Bugarín, B. V. Dorrío, C. López, J. M. Alén, M. Pérez-Amor, and J. L. Fernández, "Transient deformation measurement by double-pulsed-subtraction TV holography and the Fourier transform method", Applied Optics (in press).

18 D. Kerr, G. H. Kaufmann, and G. E. Galizzi, "Unwrapping of interferometric phase-fringe maps by the discrete cosine transform", Applied Optics 35, pp. 810-816, 1996.